

See discussions, stats, and author profiles for this publication at: <https://www.researchgate.net/publication/6751653>

# A novel cross-linked RNase A dimer with enhanced enzymatic properties

ARTICLE *in* PROTEINS STRUCTURE FUNCTION AND BIOINFORMATICS · OCTOBER 2006

Impact Factor: 2.63 · DOI: 10.1002/prot.21144 · Source: PubMed

---

CITATIONS

14

---

READS

21

5 AUTHORS, INCLUDING:



**Brigitte Simons**

AB SCIEX

16 PUBLICATIONS 266 CITATIONS

SEE PROFILE



**Harvey Kaplan**

Dehydrovax Inc.

80 PUBLICATIONS 1,385 CITATIONS

SEE PROFILE



**Terry D Cyr**

Health Canada

89 PUBLICATIONS 1,242 CITATIONS

SEE PROFILE



**Mary Alice Hefford**

Health Canada

55 PUBLICATIONS 751 CITATIONS

SEE PROFILE

# A Novel Cross-linked RNase A Dimer With Enhanced Enzymatic Properties

Brigitte L. Simons,<sup>1,2</sup> Harvey Kaplan,<sup>2</sup> Sylvie M. Fournier,<sup>1</sup> Terry Cyr,<sup>1</sup> and Mary Alice Hefford<sup>1\*</sup>

<sup>1</sup>Centre for Biologics Research, Biologics and Genetics Therapies Directorate, Health Canada, Ottawa, Ontario, Canada, K1A 0L2

<sup>2</sup>Department of Chemistry, University of Ottawa, D'Iorio Hall, 10, Marie-Curie, Ottawa, Ontario, Canada, K1N 6N5

**ABSTRACT** A new cross-linked ribonuclease A (RNase A) dimer composed of monomeric units covalently linked by a single amide bond between the side-chains of Lys<sub>66</sub> and Glu<sub>9</sub> is described. The dimer was prepared in the absence of water by incubating a lyophilized preparation of RNase, sealed under vacuum, in an oven at 85°C. It was determined that the *in vacuo* procedure does not induce any significant conformational changes to the overall structure of RNase A, yet the amide cross-link has an increased acid lability, indicating that it is exposed and conformationally strained. Examination of X-ray crystallographic structures indicates that Lys<sub>66</sub> and Glu<sub>9</sub> are not close enough for the *in vacuo* dimer to adopt any of the known domain-swapped conformations. Therefore, the *in vacuo* RNase A dimer appears to be a novel dimeric structure. The *in vacuo* RNase A dimer also exhibits a twofold increase in activity over monomeric RNase A on a per monomer basis. This doubling of enzymatic activity was shown using dsRNA and ssRNA as substrates. In addition to this enhanced ability to degrade RNA, the dimer is not inhibited by the cellular ribonuclease inhibitor protein (cRI). *Proteins* 2007;66:183–195. © 2006 Wiley-Liss, Inc.

**Key words:** ribonuclease A; *in vacuo*; enzymatic activity; covalent cross-linking; dimer

## INTRODUCTION

Bovine pancreatic ribonuclease A (RNase A) is one of the most extensively studied and characterized proteins. It, like most other members of the RNase superfamily, is a monomeric protein; however, in 1962, Crestfield et al.<sup>1</sup> observed that stable, dimeric forms of bovine pancreatic RNase A could be formed by lyophilization from a concentrated solution of 50% acetic acid. In 1967, he and his colleagues demonstrated that these noncovalent RNase A dimers were two monomeric units that had exchanged their N-terminal segments, thus forming a domain-swapped conformation<sup>2</sup> similar to that observed many years later in bovine seminal ribonuclease (BS-RNase),<sup>3</sup> a uniquely homodimeric ribonuclease. More recently, many groups have undertaken the characterization of noncovalent RNase A dimers generated by Crestfield's method.<sup>4–7</sup> Rather than a single dimeric RNase A species, recent work

had shown that RNase A dimers can exist in two distinctly different conformers: the N-terminal  $\alpha$ -helix-swapped dimer and the C-terminal  $\beta$ -strand-swapped dimer.<sup>8,9</sup> The N-terminal  $\alpha$ -helix (residues 1–15)-swapped conformer can be separated from the more dominant C-terminal  $\beta$ -strand (residues 116–124)-swapped conformer by cation exchange chromatography.<sup>5,9–11</sup> Both the N- and C-terminal domain-swapped dimers show increased catalytic activity toward dsRNA substrates.<sup>5,10</sup>

The observation that the dimeric forms of RNase are cytotoxic<sup>12</sup> has been of considerable interest as they may have applications as a therapeutic agent in preventing some types of cell proliferation (see Refs. 13 and 14, and references cited therein). BS-RNase and onconase, an amphibian RNase, are also highly cytotoxic, and both have been shown to retain activity in the presence of the cellular inhibitor, cytosolic ribonuclease inhibitor (cRI).<sup>15</sup> This ability to evade inactivation by cRI has been linked to the cytotoxic and antitumor activities<sup>16</sup> of BS-RNase, and onconase and, by extension, to other homologues of RNase A.<sup>17</sup> In solution, BS-RNase forms an equal mixture of two distinct conformers,<sup>17,18</sup> both of which are composed of two identical monomers linked by two disulfide bonds. In one of the two dimeric conformers, the two monomeric subunits appear to fold independently of one another. The other dimeric conformer, however, is assembled by the exchange of the N-terminal  $\alpha$ -helix between subunits, a process that is commonly termed 3D domain swapping.<sup>19</sup> The noncovalent dimers first identified by Crestfield are also domain-swapped dimers. However, it has recently been demonstrated that cRI strongly binds to and inhibits noncovalent, domain-swapped RNase dimers.<sup>20</sup> It therefore appears that either some other property of the RNase dimers is responsible for the cytotoxicity or, as argued by Sica et al.,<sup>21</sup> a properly formed dimeric structure can evade cRI but must be stable in the reducing environment of the cytosol to do so.

Grant sponsor: National Sciences and Engineering Research Council (NSERC).

\*Correspondence to: Mary Alice Hefford, Centre for Biologics Research, Biologics and Genetics Therapies Directorate, AL: 2201C, Health Canada, Ottawa, ON, Canada, K1A 0L2. E-mail: mary\_hefford@hc-sc.gc.ca

Received 27 January 2006; Revised 13 April 2006; Accepted 30 May 2006

Published online 16 October 2006 in Wiley InterScience (www.interscience.wiley.com). DOI: 10.1002/prot.21144

Because domain-swapped RNase A dimers are metastable and revert to monomers without the cytotoxic activity, several strategies for producing stable and/or covalent dimers have been investigated, including protein modeling from BS-RNase sequences,<sup>4</sup> covalent dimerization,<sup>22–24</sup> and numerous variants produced by site directed mutations of monomeric RNase A.<sup>7,25</sup>

We have recently developed a novel method for preparing covalently linked protein dimers from their monomers.<sup>26</sup> The cross-linking process is carried out *in vacuo* on the lyophilized protein and results in zero-length amide cross-link formed by condensation of a lysine amino group on one monomer and an aspartic or glutamic carboxyl group on the other. Because RNase has been so extensively studied and characterized, it was chosen as a test protein in the development of the methodology. A covalent RNase A dimer was observed and isolated and on further analysis was found to contain a single, zero-length covalent cross-link between a primary amino group on a lysine residue and the carboxylic acid side chain of either a glutamic or aspartic residue. In light of the therapeutic potential of dimeric RNase species, we now describe the characterization of this covalently cross-linked RNase A dimer produced by the *in vacuo* method to determine if it has the stability, enzymatic activity, and resistance to inhibition by ribonuclease inhibitor (RI) that other RNase dimers exhibit and to ascertain if we have captured covalently one of the known domain-swapped dimers or have indeed produced a new dimer of novel structure.

## EXPERIMENTAL PROCEDURES

### *In Vacuo* Cross-Linking of RNase A

Bovine pancreatic RNase A (Type I-A) was obtained from Sigma-Aldrich (Oakville, Ontario, Canada) (Lot no. 41K7655, R4875), was reconstituted in distilled water to a concentration of 5 mg/mL, and the pH of the solution was adjusted to 7.0 with 1 N NaOH. The protein solution was placed in glass tubes and lyophilized. These glass tubes were sealed under a vacuum of ~50 mtorr and then incubated in an oven at 85°C for 96 hr. The vacuum was released and the protein sample reconstituted with 40 mM NaH<sub>2</sub>PO<sub>4</sub> at pH 6.67 to give a final protein concentration of 5 mg/mL.

### Purification of RNase A Dimers

RNase A dimers were purified by two chromatography steps. The first step was size-exclusion chromatography, which was carried out using two Superdex 75 HR 10/30 columns (Amersham Biosciences, Baie, D'Urfée, PQ, Canada) attached, in tandem, to a Pharmacia FPLC system P-500 (Amersham Biosciences) with detection at 210 nm. Mobile phase (0.2 M Na<sub>2</sub>HPO<sub>4</sub> and 0.15 M NaCl at pH 6.55 at 4°C) was used at a flow rate of 0.05 mL/min and 0.5 mL fractions were collected [Fig. 1(A)]. Molecular weight standards [phosphorylase b, 94 kDa; bovine serum albumin (BSA),

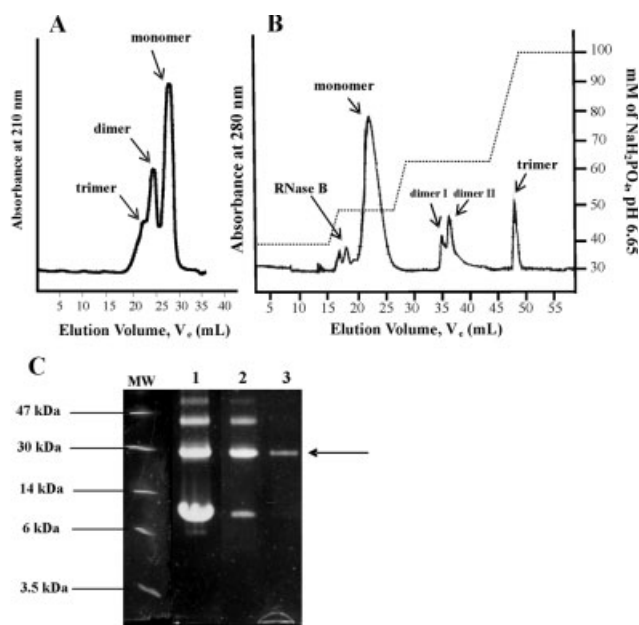


Fig. 1. Size exclusion and strong cationic exchange chromatography of uncross-linked and *in vacuo* cross-linked RNase A. Separation of *in vacuo* cross-linked RNase A (A) by size was achieved with two Superdex G75 HR 10/30 G75 columns attached in tandem using a mobile phase of 0.2 M Na<sub>2</sub>HPO<sub>4</sub> and 0.15 M NaCl at pH 6.55. (B) Large molecular weight fractions collected from SEC were then further separated by a strong cationic exchange source 15S column and elution of monomer, dimer, and trimer was achieved by a stepwise gradient of NaH<sub>2</sub>PO<sub>4</sub> between 40 and 100 mM (as indicated by the dotted line) and eluted products are as indicated. (C) 16.5% SDS Tricine gel electrophoresis of *in vacuo* total cross-linked mix of RNase A (lane 1), RNase A dimer isolated by size exclusion FLPC (lane 2), and RNase A dimer separated by cationic exchange FLPC (lane 3). RNase A *in vacuo* cross-linked dimer is indicated by the arrow.

67 kDa; ovalbumin, 43 kDa; bovine erythrocytes carbonic anhydrase, 29 kDa; trypsin inhibitor, 20.1 kDa;  $\alpha$ -lactalbumin, 14.4 kDa] used in column calibration were purchased from Sigma-Aldrich. Pooled fractions containing RNase A dimer were concentrated to 0.5 mL and the buffer was exchanged to 40 mM NaH<sub>2</sub>PO<sub>4</sub> at pH 6.67 using Amicon<sup>®</sup> Ultra 5 kDa MWCO centrifugal filtering devices (Millipore, Nepean, Ontario, Canada) with several washing cycles.

The second chromatography step was necessary to ensure that no noncovalent dimer was eluting with and contaminating the covalent dimer sample, and this was performed using a strong cation exchange Source 15S resin (Amersham Biosciences) and an 8-mL column (Bio-Rad Laboratories, Mississauga, Ontario, Canada) attached to the same FPLC system (Amersham Biosciences) at room temperature. The running buffer used was 40 mM NaH<sub>2</sub>PO<sub>4</sub> at pH 6.67 at a flow rate of 1 mL/min. Approximately 3 mg of the protein collected from the size exclusion column was loaded onto the column at 1 mL/min, and monomer, dimer, and trimer were eluted and collected in this respective order by a stepwise sodium phosphate linear gradient: 40 mM to 200 mM NaH<sub>2</sub>PO<sub>4</sub> at pH 6.7 over 1 hr as indicated in Figure 1(B). Dimeric RNase A was then collected and concentrated by Amicon<sup>®</sup> Ultra 5 kDa MWCO

centrifugal filtering devices to a volume of approximately 1 mL. Samples were kept in 40 mM  $\text{NaH}_2\text{PO}_4$  at pH 6.67 at 4°C until needed.

The concentration of the *in vacuo* cross-linked RNase A dimer present in each sample was estimated spectrophotometrically by the BCA protein quantification method.<sup>27,28</sup> Briefly, solutions of unknown protein concentration and six standard protein solutions of BSA of concentrations ranging between 0 and 5 mg/mL were reacted with bicinchoninic acid and copper sulfate 50:1 (v/v) ratio for 30 min at 37°C. The solutions were transferred into 2-mL disposable cuvettes and their absorbance at 562 nm was measured using a Beckman DC530 spectrophotometer (Beckman Coulter, Mississauga, Ontario, Canada). Protein concentrations in the samples were estimated from interpolation of the standard curve obtained for the BSA solutions.

### Acid Lability of the Amide Cross-Link in the RNase A Dimer

The mixture of cross-linked RNase A dimer and monomer present after lyophilization and incubation (1 mg samples) was reconstituted to 200  $\mu\text{L}$  in one of the following acid solutions: 0.1% (v/v) trifluoroacetic acid (TFA), 1% (v/v) TFA, 0.2% (v/v) formic acid (FA), 2% (v/v) FA, 5% (v/v) FA, and 10% (v/v) FA. Samples were incubated at 50°C for 3 hr, then neutralized with 1.0 N NaOH. A 5- $\mu\text{L}$  aliquot (5  $\mu\text{g}$  total protein) was taken from each sample, added to 10  $\mu\text{L}$  of SDS loading buffer, then run on a 16.5% Tricine SDS-PAGE at 130 V for 80 min, and stained with Coomassie Blue for visualization.

### Thermal Denaturation of RNase A Monomer and Dimer

A Jasco®810 circular dichroism (CD) spectrometer (Jasco, Easton, MD) was used to monitor the far-UV region (180–260 nm) to assess the secondary structures and thermal stability of the RNase A monomer and dimer. Samples contained 0.5 mg/mL of protein in 25 mM sodium phosphate buffer, pH 7.2, and were placed in a cell of 0.2 cm optical path. In the thermal denaturation experiments, spectra were recorded at 5°C increments as the sample was heated from 25 to 95°C and each spectrum represents the average of five accumulations. The molar ellipticities at 222 and 208 nm were monitored at each temperature. The fraction of unfolded RNase A molecules was calculated by Eq. (1),<sup>29</sup> where  $y_{\text{folded}}$  is the molar ellipticity at 222 nm at 25°C (where the protein is expected to be fully folded),  $y_{\text{temp}}$  is the molar ellipticity at 222 nm at each temperature increment, and  $y_{\text{unfolded}}$  is the molar ellipticity at 222 nm at 95°C (where the protein is expected to be fully unfolded). The  $y_{\text{temp}}$ ,  $y_{\text{folded}}$ , and  $y_{\text{unfolded}}$  were also retrieved from the molar ellipticity data collected at 208 nm. An average of these quotients, as shown in Eq. (1), gives an estimate of the fraction of folded molecules for RNase A.<sup>29</sup> The % unfolded was plotted

against temperature to estimate the melting temperature ( $T_M$ ) of the protein.

% unfolded

$$= \left( \frac{(y_{\text{folded}} - y_{\text{temp}})_{222 \text{ nm}}}{(y_{\text{folded}} - y_{\text{unfolded}})_{222 \text{ nm}}} + \frac{(y_{\text{folded}} - y_{\text{temp}})_{208 \text{ nm}}}{(y_{\text{folded}} - y_{\text{unfolded}})_{208 \text{ nm}}} \right) / 2 \quad (1)$$

Equation 1 shows percent unfolded calculation from molar ellipticity values taken at 222 and 208 nm at each 5°C incremental increase.

Ribonuclease activity was determined by the standard Kunitz assay using double stranded RNA, poly(A)–poly(U), as the substrate.<sup>30</sup> One Kunitz unit of activity corresponds to the initial change in absorbance at 260 nm under first order kinetics (i.e., linear portion of the  $A_{260}$  against time curve) divided by the total measurable increase at 260 nm measured after completion of the reaction [refer to Eq. (2)]. Enzyme solutions at a concentration of 50  $\mu\text{g}/\text{mL}$  were prepared in Kunitz buffer (0.15 M NaCl, 0.015 M citrate, pH 7.5). After the poly(A)–poly(U) substrate solutions (at concentrations varying from 4 to 80  $\mu\text{g}/\text{mL}$ , in 0.15 mL of Kunitz buffer) were equilibrated at 25°C for 30 min, an aliquot of enzyme solution (0.05 mL) was added to each giving a final reaction volume of 0.2 mL. The same reaction, with buffer rather than enzyme addition, was used as a blank for correction at each substrate concentration. The absorbance at  $A_{260}$  was monitored over 3 hr on a Tecan®SPEC-TRAFluorPlus multifunction microplate reader (Tecan US, Durham, NY). After subtraction of the appropriate blanks, the kinetic analysis of each reaction was determined by nonlinear regression analysis of the data using Sigma-Plot®(Systat Software, Point Richmond, CA). The resulting hyperbolic curves were plotted in Microsoft Excel®(Microsoft Canada, Mississauga, Ontario, Canada). The number of “Kunitz units” per mg of enzyme used is equivalent to the  $k_{\text{cat}}/K_M$  and assesses the specific activity of the enzyme, as shown in Eq. (3).

$$\text{Kunitz unit} = \frac{dA/dt}{\Delta A} \quad (2)$$

Equation 2 shows Kunitz unit of ribonuclease activity, where  $dA/dt$  is the slope of the linear part of the curve and  $\Delta A$  is the maximum absorbance obtainable (i.e., the plateau of the  $A_{260}$  versus time curve).

$$k_{\text{cat}}/K_M = \left( \frac{dA/dt}{\Delta A} \right) \frac{1}{E(\text{mg})} \quad (3)$$

Equation 3 shows that the activity is measured under first-order conditions,  $k_{\text{cat}}/K_M$  calculation, where the number of “Kunitz units,” divided by the amount of enzyme in milligrams, will equal the  $k_{\text{cat}}/K_M$ .

RNase A activity was determined in the presence or absence of cRI, (Ambion Technologies, Austin, TX). The



Kunitz assay was performed as described above, except 2000 units of RI (from a stock solution of 40 U/ $\mu$ L, provided by the supplier) or an equivalent volume of buffer was added to the samples as indicated.

### Enzymatic Digestion of RNase A Dimer

Disulphide bonds in RNase A dimer and monomer were reduced and alkylated as described by McWherter et al.<sup>31</sup> Samples (~2 mg/mL) were denatured in 0.5 M Tris-HCl, 2.5 mM EDTA, 6 M guanidinium-HCl, pH 8.5 at 37°C for 1 hr. DTT was added to a final concentration of 2.5 mM, and N<sub>2</sub> was bubbled through the sample for 5 min, followed by a further incubation at 37°C for 1 hr. Iodoacetamide (final concentration: 0.3 M) was added and allowed to react, in the dark at 37°C, with the protein for 30 min. The alkylation reaction was stopped by the addition of 100  $\mu$ L (1.42  $\times 10^{-3}$  mol) of  $\beta$ -mercaptoethanol, and samples were thoroughly dialyzed against 50 mM ammonium bicarbonate (pH 8.0) to remove all excess reagents.

Trypsin (Promega, Madison, WI) was added to each RNase sample at an enzyme to substrate ratio of 1:25 (w/w), and the protein samples were allowed to digest overnight at 37°C. The samples were then heated to 100°C for 3 min, and then evaporated to near dryness (about 10  $\mu$ L) using a Vacufuge<sup>TM</sup> speed rotorvac (Eppendorf North America, Westbury, NY).

Reverse phase HPLC (RP-HPLC) was used to separate the tryptic RNase A peptides of both monomeric and dimeric samples. Trypsin-digested samples were reconstituted in the mobile phase solvent A (5% ACN, 0.1% TFA), then injected by a Waters 770E autosampler into a Waters 600E HPLC system (Waters Limited, Mississauga, Ontario, Canada) interfaced by Millennium<sup>®</sup> HPLC software into a 0.46  $\times$  30-cm C<sub>18</sub> column provided by Vydac (Grace Vydac, Hesperia, CA). A linear gradient changing from 100% mobile phase solvent A to 35% mobile phase solvent B (95% ACN, 0.1% TFA over 60 min) at a flow rate of 1 mL/min was used to elute the peptides. Peptides were collected individually and the volume of each fraction reduced to ~10  $\mu$ L by evaporation.

### Peptide Mapping by LC-Mass Spectrometry

To protonate the peptides, 0.2% FA (v/v) was added to each of the evaporated samples containing eluted fragments to give an estimated final concentration of 50 pmol/ $\mu$ L per sample. Samples were analyzed by capillary HPLC-ESI-MS with use of a Waters Q-TOF Ultima Global [Waters (Micromass<sup>TM</sup>), Mississauga, Ontario, Canada] mass spectrometer coupled to a Waters CapLC XE system. Tryptic peptides were loaded (1.0  $\mu$ L) and desalted, at a flow rate of 20  $\mu$ L/min, on a C<sub>18</sub> Pepmap trapping column (300  $\mu$ m id  $\times$  5 mm) (LC Packings Dionex, Sunnyvale, CA). The peptide mixture was eluted using an acetonitrile solvent gradient from 0 to 40% B running over 60 min followed by a second gradient from 40 to 95% B achieved in 10 min (solvent A: 98% H<sub>2</sub>O, 0.2% FA, 2% ACN; solvent B: 90% ACN, 0.2% FA). The solvent stream, flowing at a rate of 10  $\mu$ L/min, was split prior to the analytical column to achieve a flow

rate of 200 nL/min on the analytical column, an Atlantis<sup>TM</sup> Waters C<sub>18</sub> 75  $\mu$ m  $\times$  150-mm NanoEase<sup>TM</sup> column (Waters). Mass spectral data acquisitions were controlled by MassLynx<sup>TM</sup> software using automated switching between MS and MS/MS modes. The survey MS scan (1 s) was obtained over the mass range m/z 300–1200 in the positive ion mode with a cone voltage of 40 V. When the signal reached a user-defined threshold (10 counts/sec), and the isotope pattern demonstrated that the ion was multiply charged, then peptide precursor ions were selected for MS/MS scan (2 s) over the mass range m/z 50–2000. Fragmentation was performed using argon as the collision gas and with a variable collision energy profile (20–40 eV) that depended on the charge state and the mass of the precursor ion. External calibration was achieved using a daily multipoint calibration from the MS/MS of doubly charged glu-fibrinopeptide B (Sigma-Aldrich, Oakville, Ontario, Canada).

### Fluorescent Ribonuclease Activity Assay

Monomeric and *in vacuo* cross-linked dimers of RNase A were tested for ribonuclease activity using the RNase-Alert<sup>TM</sup> (Ambion, Austin, TX) ribonuclease activity assay kit. This assay is composed of a single stranded RNA substrate with a fluorescent tag that fluoresces once the RNA substrate has been cleaved by the enzyme. Each reaction was conducted in a 96-well fluorescent black microtitre plate (Corning, NY) containing 50 pmol of substrate and 200–300 pg of enzyme in TBS (20 mM Tris-HCl, 137 mM NaCl, at pH 7.2) in a total reaction volume of 50  $\mu$ L. In selected reactions, 40 units of ribonuclease inhibitor (Ambion) was added from a stock solution at a concentration of 40 units/ $\mu$ L. The catalytic activity of the enzyme was monitored by TECAN<sup>®</sup>-GENious fluorimeter (excitation filter: 485 nm; emission filter: 535 nm) (San Jose, CA) and relative fluorescent units (RFU) were measured over 90 min.

Plots of RFU as a function of time generated hyperbolic curves in which the linear portion of the curve gives the initial velocity of the enzyme, according to a first order steady state kinetics model. The specific activity of the enzyme can be calculated by using Eq. (4). The term dRFU/dt represents the slope of the linear portion of the RFU over time curve, and RFU<sub>max</sub> – RFU<sub>0</sub> is the difference in fluorescence intensity of the maximum (once the reaction is brought to completion) minus the initial measurement. This defines an activity unit according to this assay (all values are corrected for the dRFU/dt of the blank reaction, in the absence of enzyme). The specific activity, therefore, is estimated by the activity units divided by the total amount of enzyme given in pg.

$$\begin{aligned} \text{activity unit} &= \frac{d\text{RFU}}{dt} / (\text{RFU}_{\text{max}} - \text{RFU}_0) \\ \text{specific activity} &= \frac{\text{activity unit}}{E(\text{pg})} \end{aligned} \quad (4)$$

Equation 4 shows that an activity unit in the fluorescence assay is calculated by the slope of the linear portion

of the RFU over time curve divided by the difference in total fluorescent units obtainable after the reaction is brought to completion. The specific activity is, therefore, defined as the activity units divided by the amount of enzyme in pg.

## RESULTS

### Purification of the *In Vacuo* Cross-Linked RNase A Dimer

After the *in vacuo* treatment of RNase A, the dimer was separated from free monomer by a series of liquid chromatography steps. Size exclusion chromatography using a Superdex G75 HR 10/30 column, an FPLC system, and a high salt buffer was determined to be the best method of separating the bulk of the dimer [Fig. 1(A)]. The partially purified dimer preparation was subjected to a second FPLC step, a strong cation exchange column. The elution profile, shown in Figure 1(B), revealed two separated peaks eluting in a fraction that, on subsequent examination by SDS-PAGE [Fig. 1(C)], appears to contain predominantly covalently cross-linked dimer. The RNase A covalent trimer elutes last. This preparation of the covalently cross-linked dimer was used in subsequent characterization experiments including attempts to identify the site(s) of cross-linking.

It should be noted that the second purification step (cation exchange chromatography) used in preparing the covalent RNase A dimer is very similar to that used by others<sup>10,11</sup> to separate the forms of noncovalent dimer (N-dimer and C-dimer) that are produced when RNase A is lyophilized from dilute solutions of acetic acid. Indeed, our elution profile [Fig. 1(B)] is very similar to theirs in that some separation of what are presumably two dimeric forms is evident in the chromatogram. To date, there is no evidence that the two domain-swapped dimers (separated by Gotte and coworkers<sup>11</sup>) are formed when RNase A is lyophilized from anything but dilute acetic acid solutions. Park and Raines<sup>7</sup> did note the transient formation of an unstable dimer of inactive but complementary RNase A mutants at neutral pH but this latter dimer was not characterized for its behavior on cation exchange resins.<sup>7</sup> Moreover, the presence of any noncovalent dimer (or dimers) in our preparation would have been detected as a second band, at the expected molecular size of the monomer, in the subsequent denaturing polyacrylamide gel [Fig. 1(C)], particularly given the relative heights of the peaks in the chromatogram, the high loading of sample on the gel, and the sensitivity of the staining method used. No such band is detected. The presence of the dimer peak doublet might also be explained by the covalent dimerization of RNase B (the glycosylated form of RNase A) that is present as a contaminant in the commercial preparation or the production of an RNase A–RNase B heterodimer. In our earlier work<sup>28</sup> (Fig. 1), we observed the dimers of both RNase A and RNase B as separate bands when the product of the cross-linking reaction was separated by traditional SDS-PAGE. At the resolution of the tricine gel shown in Figure 1(C), however, such separation is not expected, nor is it observed.

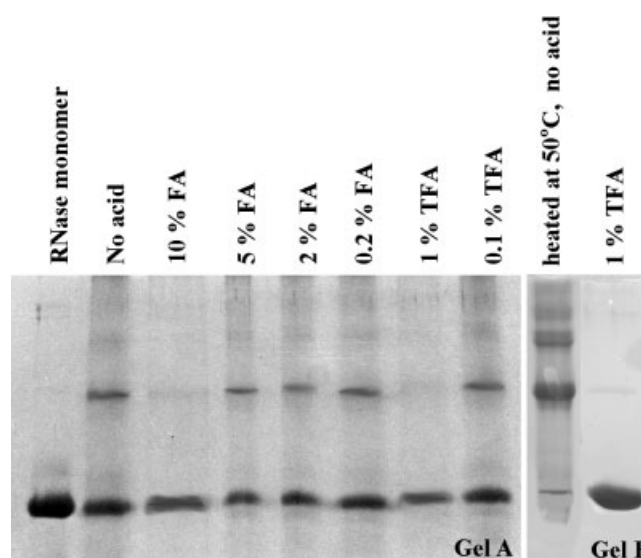


Fig. 2. 16.5% Tricine SDS-PAGE of cross-linked mixture of RNase A monomer and dimer (~5 µg total load) after hydrolysis with the acid indicated at 50°C for 3 hr (gel A). Gel B shows the purified *in vacuo* cross-linked RNase A dimer (with traces of trimer and tetramer) heated at 50°C for 3 hr in the presence and absence of 1% TFA.

### Acid Lability of the Amide Link of the RNase A Dimer

Initial efforts to locate the amide linkage in the RNase A dimer were complicated by the observation that certain techniques (such as attempts at peptide mapping using cyanogen bromide in FA or analysis by electrospray mass spectrometry with its concomitant dissolution of isolated peptides in acid for injection into the spectrometer) that were expected to differentiate dimer from monomer did not do so (data not shown). These unexpected results were tentatively attributed to loss of dimer as a result of an increased acid lability of the amide linkage between monomeric units. This hypothesis was tested by incubation of the *in vacuo* cross-linked dimer in various concentrations of trifluoroacetic acid (TFA) or FA at 50°C for 3 hr. As shown in Figure 2, incubation in 0.1% TFA does not cause dissociation of the dimer, but a 1.0% TFA solution is sufficient to break down the dimer and produce monomer. Higher concentrations of FA also break the covalent cross-link: incubation in concentrations above 5% FA results in a loss of the dimer band on the gel and an intensified monomeric band. These results indicate that amide linkages between monomeric units in the covalent dimer produced by the *in vacuo* method as well as those in larger oligomers (Fig. 2, Gel B) have a substantially higher acid lability compared with peptide bonds in the backbone chain of the monomer as no breakdown products of RNase are visible on the gel.

### Chemical and Conformational Thermal Stability of RNase A Dimer

While the amide linkage in the cross-linked dimer is unstable under moderately strong acid conditions, it is stable at neutral or slightly alkaline pH even when heated in

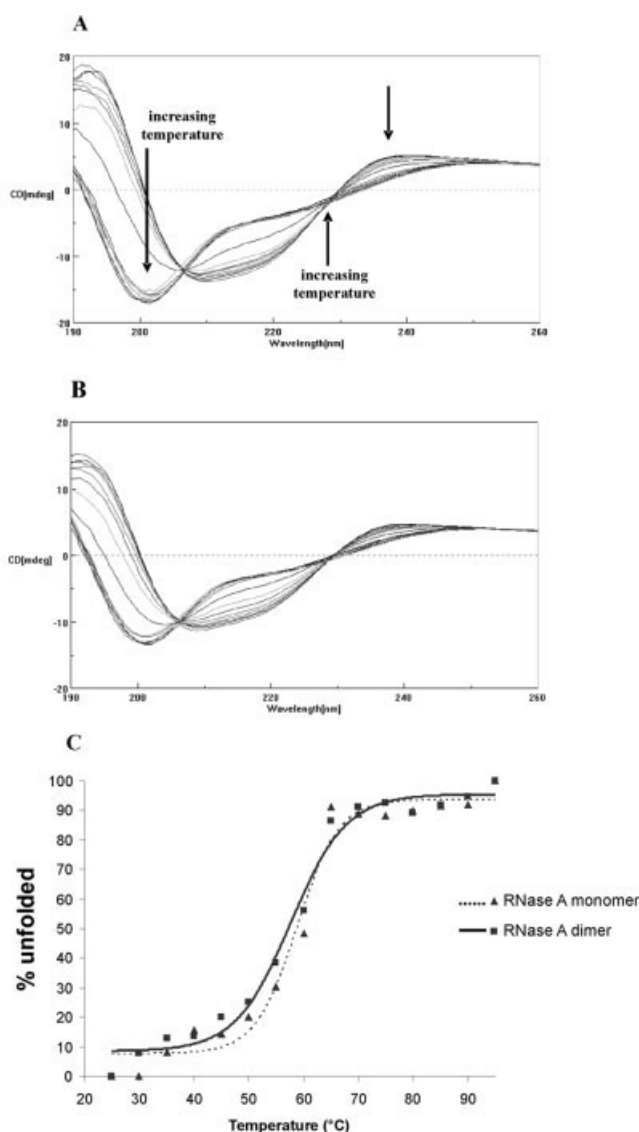


Fig. 3. Circular dichroism spectra of RNase A monomer (A) and *in vacuo* cross-linked dimer (B) measured at different temperature increments. Thermal denaturation of proteins at 0.5 mg/mL in 10 mM phosphate, pH 7.4, measured by Jasco 810 CD and spectra calculated from an average of five scans per increment in temperature. (C) Percentage of unfolded RNase A protein molecules as a function of temperature; thermal denaturation curves of RNase A monomer (dashed line) and *in vacuo* cross-linked dimer (solid line) to determine melting temperature ( $T_M$ ).

solution to 100°C under atmospheric pressure. This stability is evidenced by the fact that the sample preparation for the SDS-PAGE analysis that was initially used to reveal the presence of dimer in lyophilized protein samples involved a step of boiling the protein in denaturant for several minutes before loading on the gel. Thermal (conformational) denaturation was monitored by far-UV CD by evaluating the retention of secondary structure in the RNase A monomer and covalently cross-linked dimer as each protein was heated from 25 to 95°C.

The monomer [Fig. 3(A)] shows the expected two-state unfolding mechanism, indicated by the sharp transition in

TABLE I. Melting Temperatures of RNase A Monomer and Dimer

Ribonuclease species	Melting temperature, $T_M$ (°C)
Native RNase A <sup>31</sup>	63.2
RNase A monomer	59.8
<i>In vacuo</i> RNase A dimer	57.6

the spectra from 55 to 70°C and the isobestic point at about 208 nm.<sup>32</sup> The dimer also shows a two-state transition, though scans from 55 to 70°C indicate a slightly less abrupt transition from folded to unfolded [comparison of Fig. 3(A–C)]. The  $T_M$  values for the monomer and covalently cross-linked dimer are given in Table I, and show good agreement both with one another and with the  $T_M$  for monomeric RNase A determined by CD analysis<sup>32</sup> and confirmed by differential scanning calorimetry at concentrations of 1 mg/mL in phosphate buffered saline at pH 6.8.<sup>33</sup> In general, the thermal denaturation profiles of the RNase A monomer and covalently cross-linked dimer appear very similar, both in general shape and in the temperature at which the transition from folded to unfolded protein occurs [Fig. 3(C)], indicating that the *in vacuo* cross-linking has not significantly altered the structure of RNase A nor its folding and unfolding pathways.

### Activity of the RNase A Dimer

The ability of the covalently cross-linked dimer formed by the *in vacuo* method to cleave RNA substrates was compared with that of the RNase monomer using a well-known assay developed by Kunitz.<sup>30</sup> This method is based upon a hypochromic shift in the absorption maximum of the UV of the polynucleotide substrate, in this case, Poly(A)–Poly(U) dsRNA upon digestion to smaller fragments and the activity is determined by measuring the difference in absorbance at 260 nm as a function of time as described above. Figure 4(A) shows the effect of different substrate concentrations on the rate of change of absorbance as a function of RNase digestion time on both the dimer and monomer. Since the concentrations of both monomeric and dimeric RNase A were determined using the BCA quantification method discussed above and identical concentrations of monomer and dimer were used for comparison, the method accurately gives the relative amounts of these proteins (and therefore their relative activities) even though BSA is used to produce a standard curve. From these data and the ensuing plot of velocity against substrate concentration shown in Figure 4(B), it is apparent that the dimer (triangle points) is considerably more active toward this dsRNA substrate than the monomer (square points). The  $k_{cat}/K_M$  (per mg of protein) value obtained for the dimer is twice that of the monomer,  $0.34 \pm 0.0007$  and  $0.17 \pm 0.0007$   $\mu\text{g/mL min}^{-1} \text{mg}^{-1}$ , respectively (Table II). Thus, each monomeric unit in the covalent dimer has approximately twice the activity of a free monomer in solution.

The activity of the dimer and monomer were also evaluated in the presence of 2000 units of the cRI [Fig. 4(C)].



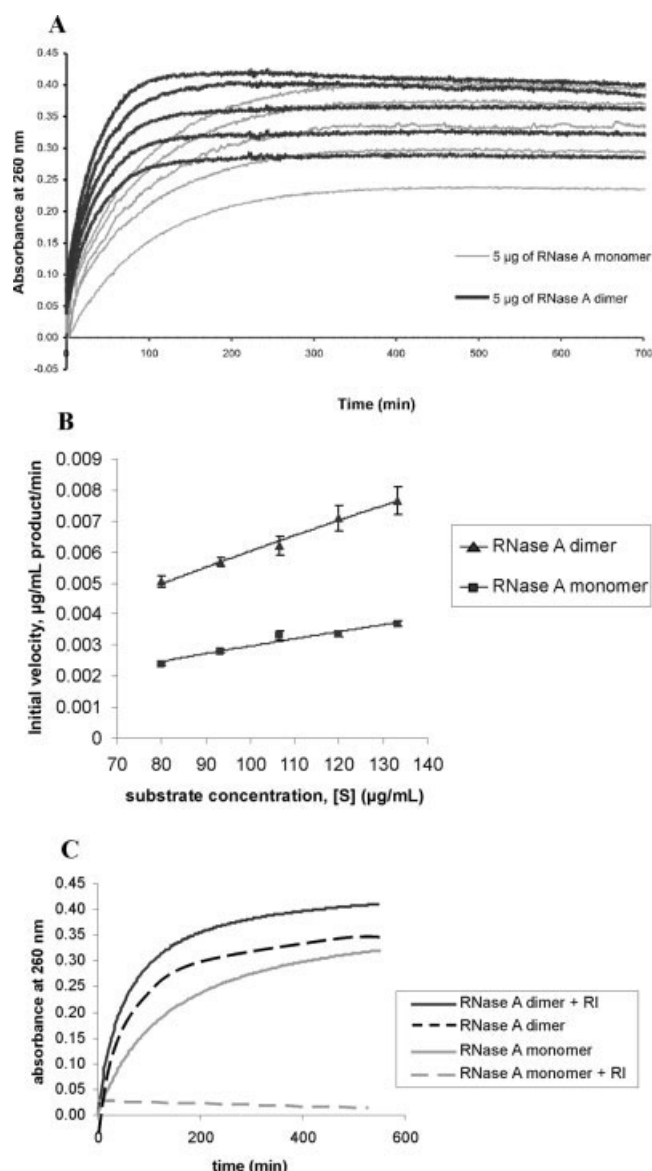


Fig. 4. Kunitz ribonuclease activity assay. (A) The difference in absorbance at 260 nm measured over time monitors the catalytic activity of 5 µg of RNase A monomer and 5 µg of the *in vacuo* cross-linked dimer toward dsRNA substrate Poly(A)–Poly(U) in amounts of 12, 14, 16, 18, and 20 µg. (B) (C) Kunitz ribonuclease activity assay in the presence of 2000 units of cytosolic ribonuclease inhibitor (RI). The difference in absorbance at 260 nm measured over time monitors the catalytic activity of 5 µg of RNase A monomer and RNase A dimer added to 20 µg of Poly(A)–Poly(U) substrate with 0 or 2000 units of RI.

The *in vacuo* cross-linked dimer with and without 2000 units of RI shows very similar slopes in the region between 0 and 80 min; if anything, the dimer appears even more active in the presence of the inhibitor than in the absence. The reaction plateaus of these curves, however, do not reach identical points. The latter observation is expected: the addition of 2000 units of RI into the reaction increases the total amount of protein in the mixture and protein molecules contribute to the overall absorbance at this wavelength, which, consequently, also increases the total obtain-

TABLE II. A Comparison Between the Specific Activities of RNase A Monomer and *In Vacuo* Cross-linked Dimer Assayed Against dsRNA Substrate

Ribonuclease A species	Kunitz units (µg/mLmin <sup>-1</sup> ) <sup>a</sup>	$k_{cat}/K_M$ Kunitz unit/mg protein <sup>b</sup>
Monomer	0.008 ± 0.0009	0.17 ± 0.0007
<i>In vacuo</i> cross-linked dimer	0.018 ± 0.0004	0.35 ± 0.000696

<sup>a</sup>Kunitz unit is calculated as an increase in absorbance per min/total measurable increase when [Poly(A).Poly(U)] = 20 µg.

<sup>b</sup>Specific activity can be estimated by the Kunitz units/mg protein or  $k_{cat}/K_M$ .

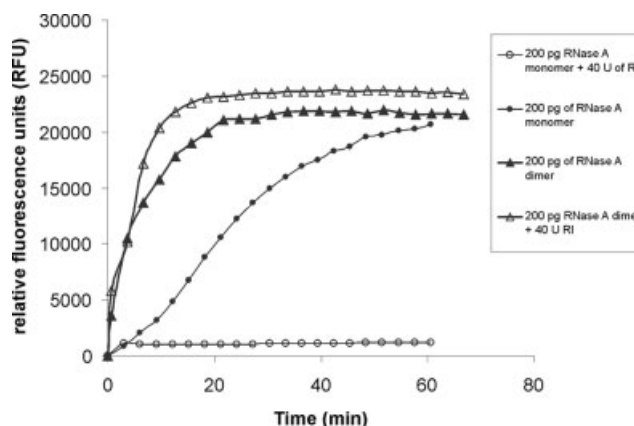


Fig. 5. Fluorescence ribonuclease assay of RNase A monomer (circle), and *in vacuo* cross-linked RNase A dimer (triangle) in the presence of cytosolic ribonuclease inhibitor (RI) (open symbols) and absence (filled symbols). Assay performed with 50 pmol of fluoro-ssRNA substrate per reaction and 40 units of RI, where indicated. Total enzyme per reaction is 200 or 270 pg in the case of ONC. Reaction was monitored using a fluorometer set at excitation/emission = 485/535 nm, readings were taken every 3 min over 1 hr.

able absorbance at 260 nm. Once again, the initial velocity of the activity curve of the RNase A monomer without RI is half that of the dimer. As expected, the addition of 2000 units of RI into the monomer activity reaction completely destroys the activity of the monomer and there is no measured increase in absorbance at 260 nm.

The activities of *in vacuo* cross-linked RNase A dimer and monomeric RNase A against a single-stranded RNA substrate were measured using an assay that monitors the fluorescence generated when a fluorescently labeled ssRNA substrate is cleaved (Ambion) (Fig. 5). A unit of activity in this fluorometric assay is defined by the rate of relative fluorescence detection over time divided by the total fluorescent counts obtainable per reaction [Eq. (4)]. The activity units, divided by the total amount of enzyme (in pg), give an estimate of the specific activity of the enzyme (Table III). From these values and the slope of the linear portion of the curves, one can conclude that the *in vacuo* RNase A dimer shows an increase in activity (compared with the activity of monomeric RNase A) toward ssRNA as well as double stranded substrates. In the presence of the cRI, monomeric



**TABLE III. Fluorescence Activity Units Over Total Amount of Enzyme in Picograms to Determine Ribonuclease Catalytic Efficiency Against a Fluoro-ssRNA Substrate**

Ribonuclease species	Units/pg enzyme (units/pg)
RNase A monomer	$1.7 \times 10^{-4}$
RNase A in the presence of RI	0
<i>In vacuo</i> cross-linked dimer	$4.2 \times 10^{-4}$
<i>In vacuo</i> cross-linked dimer in the presence of RI	$4.6 \times 10^{-4}$

RNase A is completely inactive, as shown by the flat line in Figure 5. The *in vacuo* cross-linked RNase A dimer, however, retains full activity.

### Identification the Amino Acid Side-Chains Forming the Amide Cross-Link

We have previously shown that the *in vacuo* cross-linked RNase A dimer is formed by a condensation reaction between interacting ammonium and carboxylate groups from a lysine residue and an acid residue (either aspartic acid or glutamic acid).<sup>26</sup> A peptide mapping strategy was employed to locate this amide linkage. Purified preparations of RNase A monomer and covalently cross-linked dimer were digested with trypsin (after reduction and capping of disulfides). The resulting peptides were separated by offline RP-HPLC, then identified by electrospray mass spectrometry. As we had shown that the amide cross-link is more labile than backbone amide bonds, care was taken in the choice of conditions to minimize the chance of cleaving the linkage between monomeric units. In addition, the interpretation of the results of all of these experiments took into account the possibility that the linkage between these monomeric units may have been cleaved during the derivatization processes preceding enzymatic digestion or in the sample handling in the mass spectrometric analysis.

The RP-HPLC digestion profiles of the RNase A monomer and dimer are shown in Figure 6(A, B), respectively. The 13 peaks observed in the digestion of the monomer are labeled A through N [Fig. 6(A)]. This digestion profile is the same as that obtained in peptide mapping studies<sup>31,34</sup> and accounts for the resistance to trypsin cleavage at Lys<sub>1</sub>-Glu<sub>2</sub> and Lys<sub>41</sub>-Pro<sub>42</sub> (attributed to steric hindrance resulting from the "bulky" side chains of residues following the lysine at the recognition site). In addition, the peptide containing the N-terminal glutamine (resulting from the cleavage of the Lys<sub>10</sub>-Gln<sub>11</sub> peptide bond) gives rise to two peaks, J and K, of which one is the cyclized pyroglutamic derivative. The digestion profile is also consistent with previously reported results pertaining to peak H (residues 92-98) and peak I (residues 86-98) that arise from incomplete cleavage at Arg<sub>91</sub>.<sup>31</sup> The identity of each of the labeled peaks was confirmed using mass spectrometry (data not shown) and agrees with the assignments previously made.<sup>31,34</sup>

Chemical evidence previously published<sup>26</sup> implicates the  $\epsilon$ -amino of a lysine residue in the amide link joining mono-

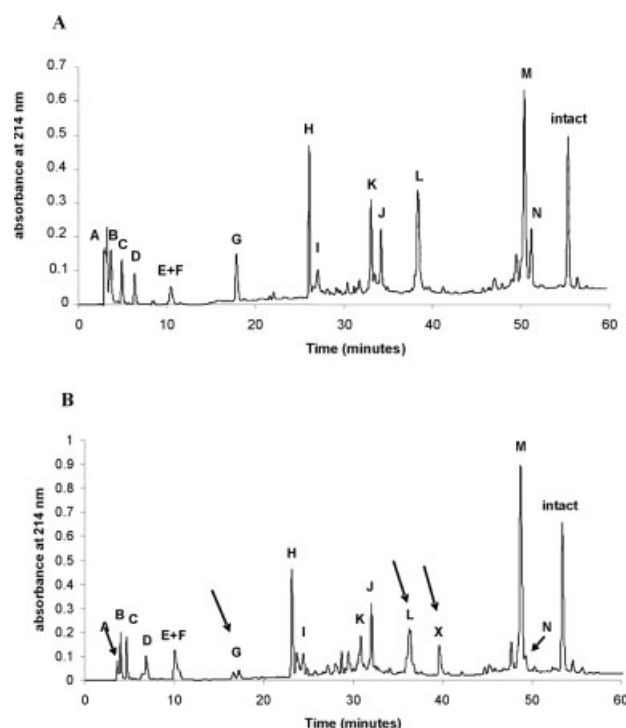


Fig. 6. Tryptic peptide map of S-carboxymethylated native monomeric RNase A (A) and S-carboxymethylated *in vacuo* cross-linked RNase A dimer (B). Peptides from the tryptic digest were separated on a  $0.46 \times 30$ -cm C<sub>18</sub> reverse phase column using solvent systems A (5% ACN, 0.1% TFA) and B (95% ACN, 0.1% TFA). A linear gradient of 0–35% B from 5 to 65 min was employed. The flow rate was 1 mL/min and the column effluent was monitored at 214 nm. The arrows indicate the reduction in height of peak G and L, as well as, the appearance of peak X in the dimer tryptic digest.

meric units. One would expect, therefore, that, in the dimer, this lysine residue will no longer be cleaved by trypsin and the abundance of peptide fragments on the C- and N-terminal sites of this lysine residue will be reduced by one half since cleavage at this site can still take place on the other monomeric unit in the dimer. Similarly, the peak representing the tryptic peptide containing the acid functionality of the amide link will also decrease by one half as this peptide from one of the monomeric units is now covalently attached in the formation of a new cross-linked peptide. In addition, the cross-link is expected to produce a new peak in the elution profile, comprised of the uncleaved lysine fragment and the covalently linked fragment containing the acid residue.

Differences in the monomeric and dimer tryptic digestion profiles are shown by the arrows in Figure 6(B). The height of the peak labeled "G" in the dimer digestion profile appears to have decreased relative to its height in the profile of the monomer. Peak "L" also appears to have decreased in height. A new peak is observed, labeled peak "X," eluting at 40 min. Mass spectrometry identified peptide G as the tripeptide: Phe-Glu-Arg that contains a potential carboxylic acid component for the amide cross-link. Peptide F, the peptide preceding L in the RNase A primary structure, contains the lysine presumed to be con-

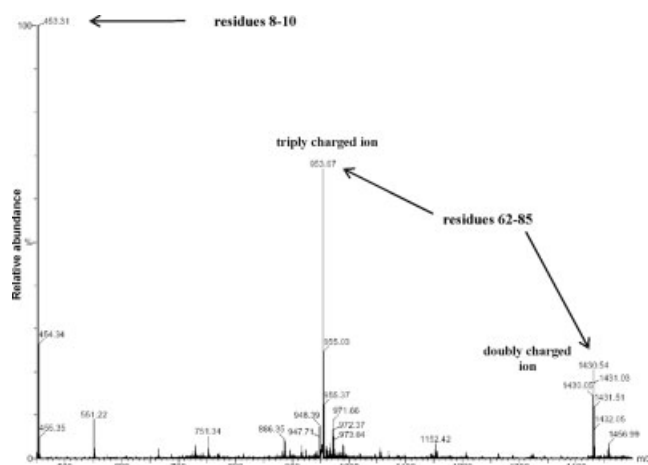


Fig. 7. Electrospray ionization TOF mass spectrum of the eluted peak "X" from the tryptic digestion profile of the *in vacuo* cross-linked RNase A dimer collected from RP-HPLC. The mass peak of  $453.3^+ \pm 1$  m.u. corresponds to residues 8–10 of the native RNase A sequence and mass peaks at  $953.6^{+++}$  and  $1430.5^{++}$  both deconvolute to the same peptide containing residues 62–85 of the native RNase A sequence.

tained in the cross-link. Peptide F is also expected to be reduced in abundance. However, the coelution of peptide F with peptide E makes any decrease in peak height difficult to observe.

### Mass Spectrometric Analysis of the *In Vacuo* Cross-Linked Peptide

On the basis of the inspection of the tryptic profiles, we predict that peak X is composed of peptides G (containing Glu<sub>9</sub>) and peak F + L (containing Lys<sub>66</sub>) cross-linked through an amide bond to give a new peptide with a predicted mass of 3292. The new peak X in the dimer profile was, therefore, eluted and analyzed by ESI-TOF-MS. The resultant spectrum (Fig. 7) shows three dominant peaks: a singly charged ion of mass 453.3, a triply charged ion of mass 953.6, and a doubly charged ion of mass 1430.5. The mass of  $453.3 \pm 1$  m.u. corresponds to the mass of the tripeptide of peak G, the glutamate-containing peptide, and is singly charged as expected. The triply charged ion at 953.6 and doubly charged ion at 1430.5 result from a single peptide of average mass  $2858.8 \pm 1$  m.u., which is the expected mass of the lysine-containing (peptide F + L, residues 62–85). The identity of this F + L peptide was confirmed by peptide sequencing using tandem MS (data not shown). The dominance of the component peptides (the glutamate-containing peptide, G, and the lysine-containing peptide, F + L) indicates that the acidic conditions (required to ensure the positive charge and ionization) and the high voltages (required for subsequent vapourization) of the mass spectrometric analysis cause cleavage of the amide cross-link in peptide X.

The assignment of a Lys<sub>66</sub>–Glu<sub>9</sub> cross-link is further strengthened by close examination of the deconvolution of the ESI-TOF-MS spectrum of peak X (see Fig. 8). The deconvoluted spectrum shows a peak of  $2858 \pm 1$  m.u.,

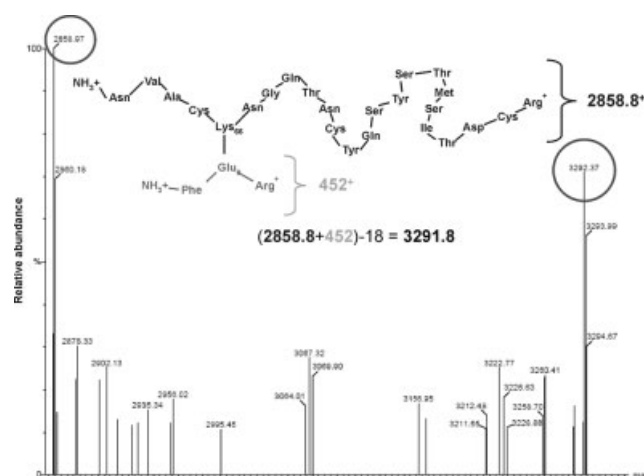


Fig. 8. Deconvoluted electrospray ionization TOF mass spectrum of the eluted peak "X" from the tryptic digestion profile of the *in vacuo* cross-linked RNase A dimer collected from RP-HPLC. The mass at  $2858 \pm 1$  m.u. corresponds to the Lys<sub>66</sub> containing fragment (sequence in bold). The intact cross-linked peptide equals  $3292.3 \pm 1$  m.u.

which corresponds to the Lys<sub>66</sub>-containing peptide, F + L. In addition, a smaller peak is detected at  $3292 \pm 1$  m.u. The observed mass of this latter peak is equal to the mass of the expected cross-link fragment: peptide F + L [which contains Lys<sub>66</sub> (2858 m.u.)] plus the mass of the Glu<sub>9</sub>-containing tripeptide (452 m.u.) minus 18 m.u. (loss of one water molecule). It appears that this latter peak corresponds to the intact cross-linked peptides that have survived the acid conditions as its mass corresponds to that predicted for sum of the masses of the two peptides involved in the amide cross-link less the mass of a water molecule lost in the condensation.

### Comparison of the Dimer Structure With Known X-Ray Crystallographic Structures of RNase A

The X-ray crystallographic structures of the N- (PBD id = 1A2W)<sup>8</sup> and C- (PBD id = 1F0V)<sup>9</sup> dimers were examined using SETOR, a visualization program developed by Evans.<sup>35</sup> The side chain of Lys<sub>66</sub> was highlighted on one of the monomeric units and the side chain of the Glu<sub>9</sub> residue on the other, and the distance between these two groups was determined (Fig. 9). In the domain-swapped N-dimer [Fig. 9(A)], the distance between Lys<sub>66</sub> and Glu<sub>9</sub> is  $\sim 20$  Å. The C-dimer structure is shown in Figure 9(B); the distance between Lys<sub>66</sub> and Glu<sub>9</sub> in this conformer is  $\gg 30$  Å. Given the large distances measured between Lys<sub>66</sub> and Glu<sub>9</sub> in both domain-swapped conformers and the evidence that the *in vacuo* cross-linking requires a condensation reaction involving a preexisting salt bridge,<sup>26</sup> neither of these structures is consistent with *in vacuo* cross-linked dimer.

The distances between carboxyl and amino groups on side chains were determined to ascertain if there are any ionic interactions that could possibly form a covalent cross-link. First, the distance from each Ogamma or Odelta of a glutamic or aspartic acid in one monomer to the  $\epsilon$ -N of the

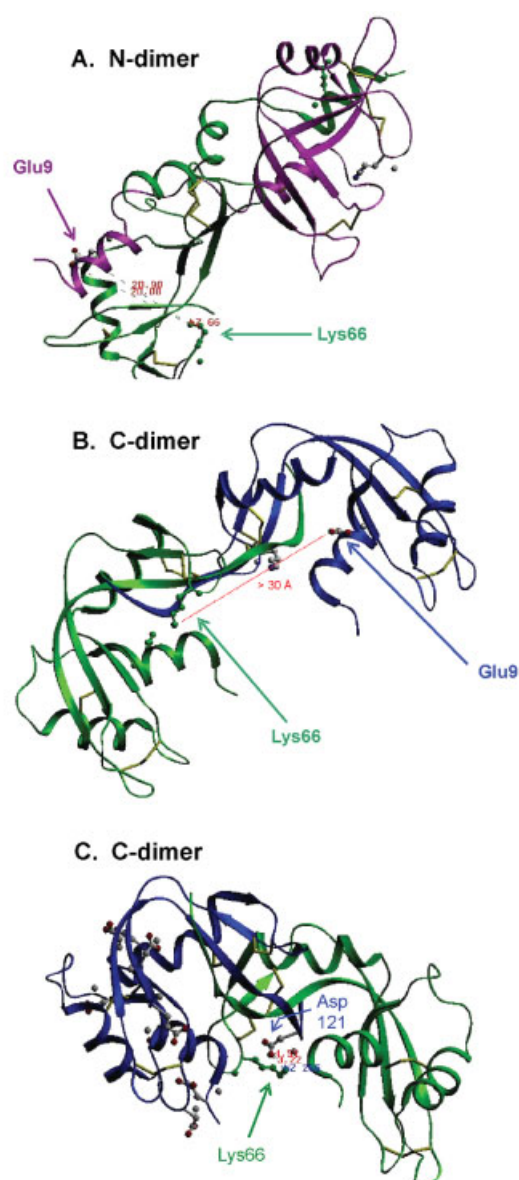


Fig. 9. X-ray crystallographic structures of the N-terminal domain-swapped dimer (A) and the C-terminal domain-swapped dimer (B) displaying the position and distances between Lys<sub>66</sub> and Glu<sub>9</sub>. Structures (N-dimer PBD id = 1A2W and C-dimer PBD id = 1F0V) are viewed by SETOR.<sup>35</sup> (C) A representation of a possible salt linkage site at positions Asp<sub>121</sub> and Lys<sub>66</sub> between monomeric units in the C-dimer.

Lys<sub>66</sub> of the other monomer was determined. Second, the side chain of Glu<sub>9</sub> was highlighted on the first molecule and the distances between its terminal oxygen atoms and the  $\epsilon$ -amino nitrogens of all other lysine residues in the second monomeric unit were determined. Third, the distances between each side chain of glutamic or aspartic residues of one monomer to each  $\epsilon$ -amino of all lysine residues in the second were determined. After careful review of these highlighted residues, Lys<sub>66</sub> is not close to any acidic residue from the domain-swapped partner in the N-dimer (data not shown). A similar conclusion is drawn if the same examination is made using Glu<sub>9</sub> of the first monomer to any Lys res-

idue in the other (data also not shown). Examination of the C-dimer, however, reveals the possibility of salt-bridge interaction, between Lys<sub>66</sub> and Asp<sub>121</sub> [The requisite groups are at an interatomic distance of 3.22 Å, as shown in Fig. 9(C)]. If indeed the *in vacuo* procedure had produced the known C-terminal domain-swapped RNase A dimer, this salt-bridge, between Lys<sub>66</sub> and Asp<sub>121</sub>, would be expected to be the site of cross-linking. No evidence for such a linkage was found.

## DISCUSSION

We have recently developed a novel method to covalently cross-link proteins *in vacuo* in the absence of water and chemical reagents. In the course of that method development, we have produced a homogeneous covalent dimer of pancreatic RNase A in which the two monomeric units are joined by a single, zero-length (amide) linkage formed from the condensation at the side chains of a specific lysine residue and a specific acidic residue, either glutamate or aspartate.<sup>26</sup> The careful examination of peptide maps followed by mass spectrometric analysis presented here reveals an amide cross-link between the side chains of Lys<sub>66</sub> and Glu<sub>9</sub> of interacting monomeric units in the dimer produced by the *in vacuo* cross-linking procedure. A thorough review of the known crystal structures of the noncovalent N- and C-domain-swapped dimers indicates that neither of these structures can account for this observed cross-link. Likewise, the close juxtapositioning of the requisite functional groups of Lys<sub>66</sub> and Glu<sub>9</sub> on adjacent monomers in the lyophilized state to form a functional dimer is unlikely to result from the packing of one monomeric or one dimeric entity against another in a manner analogous to that seen in the packing of the unit cell of crystals.

The crystal structure of RNase A is obtained from the protein molecules initially crystallizing in a solvating environment. Because of these conditions, X-ray crystal structures of RNase A are not representative of the structure of dehydrated freeze dried protein treated *in vacuo*. Upon lyophilization, the secondary structure content of RNase A changes remarkably with a decrease in  $\alpha$ -helix and an increase in  $\beta$ -sheet.<sup>36,37</sup> The magnitude of the change is greatly dependant upon the solution conditions during lyophilization, and lyophilized RNase A has been characterized as having glass-like properties.<sup>38</sup> The differences in intermolecular packing of RNase A as a lyophilized sample compared with a crystallized lattice may account for distinctive salt bridging between interacting molecules. The examination of the X-ray crystal structures of monomeric and dimeric RNase A strongly suggests that the *in vacuo* RNase A dimer (with an amide linkage between Lys<sub>66</sub> and Glu<sub>9</sub>) does not result from a condensation reaction between interacting residues in any known crystallographic structure and that the dimer formed by the *in vacuo* procedure is indeed a new dimeric structure not previously observed.

In the absence of a detailed structure of this novel RNase A dimer produced by the *in vacuo* method, the reasons for the specificity of the cross-link and the involvement of the specific residues remains speculative. To our knowledge,



neither Lys<sub>66</sub> nor Glu<sub>9</sub> have been noted as particularly reactive residues. Glu<sub>9</sub>, however, appears to be somewhat exposed in X-ray structures of RNase A monomers. Indeed, Ferodov and coworkers<sup>39</sup> observed a salt-linkage between Glu<sub>9</sub> on one molecule of RNase A in the crystal structure unit cell and the  $\epsilon$ -amino group of Lys<sub>61</sub> on an adjacent monomer. Lys<sub>66</sub>, on the other hand, has been identified as occupying the p<sub>0</sub> subsite positing in the binding cleft of RNase A monomers and recently has been shown to help dictate the specificity (endo or exo) of cleavage.<sup>40</sup> The p<sub>0</sub> site, however, is considered the least important of the three major binding sites (p<sub>1</sub>, p<sub>2</sub>, p<sub>0</sub>) and is not required for catalytic activity as modification of this residue in monomeric RNase A results in only a modest decrease in enzymatic activity.<sup>41</sup> Given these data and the fact that only one of the two Lys<sub>66</sub> residues in the *in vacuo*-produced dimer is involved in cross-linking, it is perhaps not surprising that this novel, covalently cross-linked dimer retains activity. (see later).

Recent evidence that other RNase dimers exhibit enhanced catalytic activity toward dsRNA substrates and a modulated biological activity *in vivo* as well as cytotoxicity and antitumor activity<sup>13,25</sup> have prompted a more detailed characterization of the properties of the *in vacuo* cross-linked dimer. While noncovalent dimers are only metastable in solution and can be readily and irreversibly converted to monomer on heating,<sup>2,42</sup> the covalent dimer produced by *in vacuo* cross-linking is stable both in longer term storage [either frozen or at 4°C (data not shown)] and upon heating, even to 100°C. It is also stable in neutral and basic solutions (data not shown) but unstable in certain acidic conditions (Fig. 2). The increased acid lability, relative to backbone peptide bonds, may be due to strain: a single amide bond, which is presumably fully exposed, links two bulky monomeric units. Acid lability of strained bonds is not surprising; indeed the amide linkages between aspartic acid and proline residues are sensitive to acid hydrolysis when incubated, without heating, at pH 2.<sup>43</sup> The amide cross-link also appears to be labile under conditions used in ionization for mass spectrometric analysis. This is not unexpected as strained bonds have been shown to have chemical instabilities under gas phase acidic vaporization induced by mass spectrometric methods.<sup>44,45</sup> The covalent cross-linking of RNase A using the *in vacuo* method does not appear to affect the overall fold of the monomeric units as evidenced by the CD studies (Fig. 3) and the observed retention and enhancement of enzymatic activity (discussed below). It does, however, unexpectedly result in a dimer with slightly less thermal stability and a less cooperative unfolding transition than the monomer. This result may indicate that the dimer is slightly less tightly packed than the monomer alone and is consistent with the conclusion that the covalent dimer produced by the *in vacuo* method is not a covalent form of one of the intercalating dimers formed by lyophilization out of acetic acid.

Previous studies with noncovalent dimers of RNase A<sup>5,7,10</sup> and covalent dimers produced by conventional chemical cross-linking reactions in solution<sup>23</sup> indicate that the dimerization of RNase A can result in changes to the enzy-

matic behavior of the protein, changes that make dimeric RNases potential therapeutic agents. Increased activity of RNase A dimers against dsRNA was observed by several groups,<sup>5,7,8,10</sup> a phenomenon attributed to a presumed destabilization effect on polynucleotide substrates from an increase in surface positive charge density on the dimer molecule acting upon the negatively charged backbone of RNA.<sup>46</sup> Data presented in Figures 4 and 5 indicate that the RNase A dimer produced by the *in vacuo* cross-linking procedure is also more active toward dsRNA substrates, in fact, twice as active on a per monomer basis as monomeric RNase A. Of particular note is the ability of the *in vacuo* cross-linked dimer to catalyze the degradation of a ssRNA substrate (Fig. 5), a property that the noncovalent, domain-swapped dimers produced by lyophilization from acetic acid do not have. In fact, Park and Raines<sup>7</sup> report that the acid lyophilized noncovalent dimer displayed a fourfold decrease in specific activity toward poly(cytidylic acid), a single stranded polyribonucleic acid polymer. The retention of at least full catalytic activity of the dimer reinforces the conclusion<sup>26</sup> that the *in vacuo* method of cross-linking retains the structure or function of the proteins being treated.

The *in vacuo* cross-linked RNase A dimer is resistant to inhibition by cRI [Fig. 4(C)]. This resistance to inhibition by cRI was also observed by RNase A dimeric derivatives prepared by the chemical cross-linking of RNase A using the bifunctional reagent dimethyl suberimidate<sup>23,24</sup> and for the cytotoxic but monomeric RNase A analogue, oconase.<sup>47</sup> Others have proposed that, once inside the cell, cRI binds with monomeric RNase A and that it is this interaction which prevents the catalytical degradation of RNA.<sup>16</sup> This regulatory mechanism can also be defeated by the naturally dimeric form of BS-RNase.<sup>17</sup> Monti and D'Alessio have recently proposed that it is the sheer size of the dimeric form of BS-RNase that prevents it from binding and interacting with the large horseshoe-like structure of cRI.<sup>48</sup> The hypothesis that a similar ability to evade cRI is also responsible for the cytotoxicity of noncovalent, domain-swapped RNase A dimers has also been advanced,<sup>14</sup> an argument based at least in part on the size of the domain-swapped moieties and some molecular modeling studies.<sup>6</sup> Recent experimental evidence, however, demonstrates that these domain-swapped dimers do indeed bind to cRI, perhaps with a separate molecule of cRI interacting with each monomeric unit of the noncovalent dimer.<sup>20</sup> Thus, while the ability to evade binding by cRI does not appear to be an absolute requirement for cytotoxicity and/or antitumor activity, at least some potent cytotoxic ribonucleases are resistant to inhibition to cRI. This resistance to inhibition is shared by the covalent dimer characterized here and should enhance the activity of these RNase moieties once present in target cell. These data, in conjunction with the activity data above, suggest that the *in vacuo* cross-linked dimer of RNase A is a novel dimeric structure that possess all the catalytic properties thought to be responsible for the desirable cytotoxic effects and antitumor activities of naturally occurring ribonuclease dimers and acetic acid lyophilized noncovalent dimeric aggregates described in the literature.



The fact that the *in vacuo* method of cross-linking produces a homogenous, covalent RNase A dimer with enhanced activity has several implications, both in terms of protein chemistry in general and in terms of the development of potential chemotherapeutic agents in particular. In the case of RNase A presented here, the *in vacuo* method reproducibly produced a single, specific cross-link as the major product and the resultant dimer retained enzymatic activity. We have described the use of the method to make other covalent cross-linked constructs including immobilized enzymes<sup>49</sup> and enzymes cross-linked to antibodies (manuscript in preparation). All of these covalent constructs retained the biological activities of the original monomeric proteins. We have also used the method to produce heterodimers of RNase A and Onconase (unpublished results). None of these constructs, however, has been as extensively characterized as the covalent RNase A dimer described here and we are unable to say whether or not the method always gives a single, unique covalent cross-link or if that characteristic is unique to the RNase A dimer. Others<sup>50</sup> have used a variation of our *in vacuo* method (which deliberately creates multiple cross-linked sites) to explore protein-to-protein interactions. Their demonstration that the cross-links produced from lyophilized proteins accurately reflect the protein-protein interactions known to occur in solution is another indication that the method does not significantly alter the native structure of the protein. It also leads one to speculate that the Lys<sub>66</sub>-Glu<sub>9</sub> interaction "frozen" in this covalent RNase dimer may reflect an interaction that is present in at least some portion of the native ensemble of molecules of RNase A present in solution.

The demonstration here that one can produce a homogenous, covalent, dimeric RNase A with desirable properties is also important to the development of therapeutic agents. If further studies demonstrate cytotoxicity, this dimeric form of RNase A has several advantages that make it amenable to use as a therapeutic agent. First, it is simple and inexpensive to produce and no chemical reagents are used in its production. Second, the dimer produced is covalent and, undermost conditions, stable. Third, it is chemically homogenous and from a mammalian source. Our results therefore justify a substantial effort to demonstrate if this molecule is cytotoxic and to determine the specificity of the cytotoxicity.

## ACKNOWLEDGMENTS

The authors thank Drs. Michel Girard, Carol Huber, and Steve Evans for use of instruments and protein modeling software (SETOR), and Corinne Hoesli and Sophie D'Aoust for their technical assistance.

## REFERENCES

1. Crestfield AM, Stein WH, Moore S. On the aggregation of bovine pancreatic ribonuclease. *Arch Biochem Biophys* 1962;Suppl 1:217-222.
2. Crestfield AM, Fruchter RG. The homologous and hybrid dimers of ribonuclease A and its carboxymethyl histidine derivatives. *J Biol Chem* 1967;242:3279-3284.
3. Mazzarella L, Capasso S, Demasi D, Di LG, Mattia CA, Zagari A. Bovine seminal ribonuclease: structure at 1.9 Å resolution. *Acta Crystallogr D Biol Crystallogr* 1993;49:389-402.
4. Di Donato A, Cafaro V, D'Alessio G. Ribonuclease A can be transformed into a dimeric ribonuclease with antitumor activity. *J Biol Chem* 1994;269:17394-17396.
5. Gotte G, Libonati M. Two different forms of aggregated dimers of ribonuclease A. *Biochim Biophys Acta* 1998;1386:106-112.
6. Sorrentino S, Barone R, Bucci E, Gotte G, Russo N, Libonati M, D'Alessio G. The two dimeric forms of RNase A. *FEBS Lett* 2000;466:35-39.
7. Park C, Raines RT. Dimer formation by a "monomeric" protein. *Protein Sci* 2000;9:2026-2033.
8. Liu Y, Hart PJ, Schlunegger MP, Eisenberg D. The crystal structure of a 3D domain-swapped dimer of RNase A at a 2.1-Å resolution. *Proc Natl Acad Sci USA* 1998;95:3437-3442.
9. Liu Y, Gotte G, Libonati M, Eisenberg D. A domain-swapped RNase A dimer with implications for amyloid formation. *Nat Struct Biol* 2001;8:211-214.
10. Gotte G, Bertoldi M, Libonati M. Structural versatility of bovine ribonuclease A. Distinct conformers of trimeric and tetrameric aggregates of the enzyme. *Eur J Biochem* 1999;265:680-687.
11. Nenci A, Gotte G, Bertoldi M, Libonati M. Structural properties of trimers and tetramers of ribonuclease A. *Protein Sci* 2001;10:2017-2027.
12. Bartholeyns J, Baudhuin P. Inhibition of tumor cell proliferation by dimerized ribonuclease. *Proc Natl Acad Sci USA* 1976;73:573-576.
13. Matousek J. Ribonucleases and their antitumor activity. *Comp Biochem Physiol C Toxicol Pharmacol* 2001;129:175-191.
14. Libonati M, Gotte G. Oligomerization of bovine ribonuclease A: structural and functional features of its multimers. *Biochem J* 2004;360:311-327.
15. Matousek J, Soucek J, Salvik T, Tománek M, Lee JE, Raines RT. Comprehensive comparison of the cytotoxic activities of onconase and bovine seminal ribonuclease. *Comp Biochem Physiol C Toxicol Pharmacol* 2003;136:343-356.
16. Haigis MC, Kurten EL, Raines RT. Ribonuclease inhibitor as an intracellular sentry. *Nucleic Acids Res* 2003;31:1024-1032.
17. Kim JS, Soucek J, Matousek J, Raines RT. Mechanism of ribonuclease cytotoxicity. *J Biol Chem* 1995;270:31097-31102.
18. Piccoli R, Tamburrini M, Piccialli G, Di DA, Parente A, D'Alessio G. The dual-mode quaternary structure of seminal RNase. *Proc Natl Acad Sci USA* 1992;89:1870-1874.
19. Bennett MJ, Schlunegger MP, Eisenberg D. 3D domain swapping: a mechanism for oligomer assembly. *Protein Sci* 1995;4: 2455-2468.
20. Naddeo M, Vitagliano L, Russo A, Gotte G, D'Alessio G, Sorrentino S. Interactions of the cytotoxic RNase A dimers with the cytosolic ribonuclease inhibitor. *FEBS Lett* 2005;579:2663-2668.
21. Sica F, Di Fiore A, Merlino A, Mazzarella L. Structure and stability of the non-covalent dimer of bovine seminal ribonuclease: an enzyme tailored to evade ribonuclease protein inhibitor. *J Biol Chem* 2004;279:36753-36760.
22. Tarnowski GS, Kassel RL, Mountain IM, Blackburn P, Wilson G, Wang D. Comparison of antitumor activities of pancreatic ribonuclease and its cross-linked dimer. *Cancer Res* 1976;36:4074-4078.
23. Gotte G, Testolin L, Costanzo C, Sorrentino S, Armato U, Libonati M. Cross-linked trimers of bovine ribonuclease A: activity on double-stranded RNA and antitumor action. *FEBS Lett* 1997;415:308-312.
24. Wang D, Wilson G, Moore S. Preparation of cross-linked dimers of pancreatic ribonuclease. *Biochemistry* 1976;15:660-665.
25. Leland PA, Schultz LW, Kim BM, Raines RT. Ribonuclease A variants with potent cytotoxic activity. *Proc Natl Acad Sci USA* 1998;95:10407-10412.
26. Simons BL, King MC, Cyr T, Hefford MA, Kaplan H. Covalent cross-linking of proteins without chemical reagents. *Protein Sci* 2002;11:1558-1564.
27. Smith PK, Krohn RI, Hermanson GT, Mallia AK, Gartner FH, Provenzano MD, Fujimoto EK, Goeke NM, Olson BJ, Klenk DC. Measurement of protein using bicinchoninic acid. *Anal Biochem* 1985;150:76-85.
28. Wiechelman KJ, Braun RD, Fitzpatrick JD. Investigation of the bicinchoninic acid protein assay: identification of the groups responsible for color formation. *Anal Biochem* 1998;175:231-237.
29. Navon A, Ittah V, Laity JH, Scheraga HA, Haas E, Gussakovskyy EE. Local and long-range interactions in the thermal unfolding

- transition of bovine pancreatic ribonuclease A. *Biochemistry* 2001; 40:93–104.
30. Kunitz M. Crystalline desoxyribonuclease. I. Isolation and general properties spectrometric method for measurement of desoxyribonuclease activity. *J Gen Physiol* 1950;33:349–362.
  31. McWherter CA, Thanhauser TW, Fredrickson RA, Zagotta MT, Scheraga HA. Peptide mapping of bovine pancreatic ribonuclease A by reverse phase high-performance liquid chromatography. I. Application to the reduced and S-carboxymethylated protein. *Anal Biochem* 1984;141:523–537.
  32. Stelea SD, Pancoska P, Benight AS, Keiderling TA. Thermal unfolding of ribonuclease A in phosphate at neutral pH: deviations from the two-state model. *Protein Sci* 2001;10:970–978.
  33. Klink TA, Raines RT. Conformational stability is a determinant of ribonuclease A cytotoxicity. *J Biol Chem* 2000;275:17463–17467.
  34. Hirs CH, Moore S, Stein WH. Peptides obtained by tryptic hydrolysis of performic acid-oxidized ribonuclease. *J Biol Chem* 1956;219:623–642.
  35. Evans SV. SETOR: hardward-lighted three dimensional solid model representations of macromolecules. *J Mol Graph* 1993;11:134–138.
  36. Griebenow K, Klivanov AM. Lyophilization-induced reversible changes in the secondary structure of proteins. *Proc Natl Acad Sci USA* 1995;92:10969–10976.
  37. Dong A, Meyer JD, Kendrick BS, Manning MC, Carpenter JF. Effect of secondary structure on the activity of enzymes suspended in organic solvents. *Arch Biochem Biophys* 1996;334:406–414.
  38. Bell JA. X-ray crystal structure of severely desiccated protein. *Protein Sci* 1999;8:2033–2040.
  39. Fedorov AA, Joseph-McCarthy D, Fedorov E, Sirakova D, Graf I, Almo SC. Ionic interactions in crystalline bovine pancreatic ribonuclease A. *Biochemistry* 1996;35:15962–15979.
  40. Cuchillo CM, Moussaoui M, Barman T, Travers F, Nogués MV. The exo- or endonucleolytic preference of bovines pancreatic ribonuclease A depends on its subsites structure and on the substrate size. *Protein Sci* 2002;11:117–128.
  41. Nogués MV, Moussaoui M, Boix E, Vilanova M, Ribó, M, Cuchillo CM. The contribution of noncatalytic phosphate-binding subsites to the mechanism of bovine pancreatic ribonuclease A. *Cell Mol Life Sci* 1998;54:766–774.
  42. Fruchter RG, Crestfield AM. On the structure of ribonuclease dimer. Isolation and identification of monomers derived from inactive carboxymethyl dimers. *J Biol Chem* 1965;240:3875–3882.
  43. Creighton TE. Chemical properties of peptides. In: *Proteins, structures and molecular properties*, 2nd ed. New York: W. H. Freeman; 1993:1–47.
  44. Yu W, Vath JE, Huberty MC, Martin SA. Identification of the facile gas-phase cleavage of the Asp-Pro and Asp-Xxx peptide bonds in matrix-assisted laser desorption time-of-flight mass spectrometry. *Anal Chem* 1993;65:3015–3023.
  45. Skribanek Z, Mezo G, Mak M, Hudecz F. Mass spectrometric and chemical stability of the Asp-Pro bond in herpes simplex virus epitope peptides compared with X-Pro bonds of related sequences. *J Pept Sci* 2002;8:398–406.
  46. Matousek J, Gotte G, Pouckova P, Soucek J, Slavik T, Vottariello F, Libonati M. Antitumor activity and other biological actions of oligomers of ribonuclease A. *J Biol Chem* 2003;278:23817–23822.
  47. Wu YN, Mikulski SM, Ardeli W, Rybak SM, Youle RJ. A cytotoxic ribonuclease: study of the mechanism of onconase cytotoxicity. *J Biol Chem* 1993;268:10686–10693.
  48. Monti DM, D'Alessio G. Cytosolic RNase inhibitor only affects RNases and intrinsic cytotoxicity cytosolic. *J Biol Chem* 2004;279:39195–39198.
  49. Taylor RH, Fournier SM, Simons BL, Kaplan H, Hefford MA. Covalent protein immobilization on glass surfaces: application to alkaline phosphatase. *J Biotechnol* 2005;118:265–269.
  50. El-Shafey A, Tolic N, Young MM, Sale K, Smith RD, Kery V. “Zero-length” cross-linking in solid state as an approach for analysis of protein-protein interactions. *Protein Sci.* 2006;15:429–440.